

Assessment of Thermal Bridging of Fasteners through Insulated Roof Assemblies

By Sarah Rentfro, PE; Georg Reichard, PhD, PE; Elizabeth Grant, PhD, AIA; Jennifer Keegan, AIA; Eric Olson, PE; Cheryl Saldanha, PE, CPHD; and Thomas J. Taylor

This paper was originally presented at the 2023 IIBEC International Convention and Trade Show.

FASTENERS THROUGH ROOFING assemblies, composed of metal screws and plates, are thermal bridges that bypass the thermal insulation and create points of increased heat flow. **Figure 1** shows an example of this effect on snow-covered roofs.

As energy code requirements for thermal insulation have become more stringent, quantifying that loss through the building enclosure due to thermal bridging has become more relevant. For this reason, some energy codes and performance standards require documenting thermal bridges and quantifying their influence through detailed analysis. The impacts of point thermal bridges (such as fasteners) can be numerically simulated with software tools; however, such simulations are often time-consuming and sometimes need laboratory tests as validation.

This study provides a relative comparison of various roofing configurations with and without fasteners. The authors compare the

thermal performance of a physical assembly, tested under controlled laboratory conditions, with a detailed three-dimensional (3-D) computer simulation of the same assembly. By incrementally increasing the complexity of the assemblies in the tests and simulations, the authors seek to better understand the limitations of simulations, with the ultimate goal of developing an experimentally validated computer simulation approach that will enable the evaluation of a broader range of roof assemblies and roof fastener configurations.

Interface articles may cite trade, brand, or product names to specify or describe adequately materials, experimental procedures, and/or equipment. In no case does such identification imply recommendation or endorsement by the International Institute of Building Enclosure Consultants (IIBEC).



Figure 1. Examples of thermal bridging at fasteners on snow-covered roofs.

The authors have approached this in two phases, the first of which is covered within this paper. This preliminary phase focused on the change in heat flux or flow (converted into a thermal resistance or *R*-value) through a series of test roof assemblies with and without fasteners. The authors did not compare surface or internal temperatures of the test assemblies to computer simulations and so cannot yet comment on the validity or accuracy of the simulations and the experimental results. The authors intend to publish a separate follow-up study comparing the experimental data to two- and three-dimensional computer simulations to review the accuracy of computer modeling methods commonly used for calculating and accounting for thermal bridges in the design and construction industry.

RELATED STUDIES

Several simulation studies, discussed in further detail below, have estimated the thermal penalty attributable to fasteners in roofing assemblies.

A Heat Transfer Analysis of Metal Fasteners in Low-Slope Roofs

In an early finite-difference method simulation, Burch et al.¹ found an increase of 3% to 8% in heat loss due to fasteners. They examined fasteners modeled as cylinders with metal caps in low-slope roofs with metal and wood decks at a density of 0.5 fasteners/ft² (5.4 fasteners/m²) in insulation ranging from 1 to 6 in. (25 to 150 mm) thick. The increase in heat loss rose with insulation thickness; the 8% increase in heat loss corresponded to the assembly with 6 in. of insulation. They found that burying fasteners below the top layer of insulation reduced their thermal effect to one-fourth that of the case where fasteners penetrated both layers of insulation. Further, fasteners had twice the effect in metal decks as compared to wood decks, and replacing the metal fastener caps with plastic caps reduced thermal loss per fastener by 44%.

Effects of Mechanical Fasteners and Gaps between Insulation Boards on Thermal Performance of Low-Slope Roofs

Petrie et al.² conducted laboratory experiments on roof assemblies incorporating three different types of fasteners through two 2 in. (51 mm) layers of polyisocyanurate (polyiso) insulation and found that fasteners, on average, reduced the thermal resistance of the roof assembly by 7% at a mean insulation temperature of 75°F (24°C) compared to the same roof assembly with no fasteners. Petrie et al.'s steady-state

simulation with HEATING 7 showed a 12% reduction in roof *R*-value for fasteners with steel plates, while only a 3% reduction in roof *R*-value when using specially designed steel fasteners with plastic heads extending through the top layer of insulation. Findings were extended to determine their impact on simulated heating and cooling loads in six locations representing varying climates in the US.

Roofing Research and Standards Development: ASTM STP1590

In a simulation of a roof assembly with fastener plates placed above the cover board and fasteners penetrating the insulation into a steel roof deck, Olson et al.³ found that while the system nominally met the insulation requirements of the *International Energy Conservation Code*,⁴ it failed to meet these requirements when the conductive effect of industry-standard fasteners was considered. Olson et al. showed that, in a simulated roof assembly, the thermal penalty of fasteners in a temperate climate may exceed that of other penetrations such as roof drains, equipment supports, and roof vents in a typical installation. They explained that this was due to the large number of fasteners as compared to a typically smaller number of other, larger roof penetrations.

Olson et al. used the 3-D, finite-difference software HEAT3 to find a roughly 17% increase in heat loss caused by fasteners, assuming exposed metal plates over gypsum cover board at 1 fastener per 2 ft² (0.2 m²) or 0.5 fasteners/ft² (5.4 fasteners/m²).

Olson et al. explored the protective effect of using an insulating cover board in lieu of a gypsum cover board, and also the impact of placing fasteners below the cover board and fully adhering the cover board with adhesive. Their simulations showed that even when adhering an insulating cover board over fastened insulation, there was still a 10% reduction in effective thermal resistance compared to a roof assembly with no fasteners.

Toward Codification of Energy Losses from Fasteners on Commercial Roofing Assemblies & Development of Chi-Factors Towards Codification of Thermal Bridging in Low-Slope Roofing Assemblies

Moletti and Baskaran⁵ and Moletti et al.⁶ tested a range of common roofing assemblies in a horizontal guarded hot box apparatus and found that thermal bridging attributable to

roof fasteners increased with fastener density and with increasing thermal resistance of the insulation they penetrate. They reported a loss in effective *R*-value ranging from 4.4% to 13.3% across design assemblies rated *R*-26 through *R*-36. They also found that covering the fastener heads with the top layer of insulation led to 30% to 70% reductions in thermal bridging compared to fasteners extending through the cover board and insulation, with more favorable results derived from a thicker top layer of insulation.

Building Envelope Thermal Bridging Guide V. 1.6

Developed by Morrison Hershfield⁷ and industry partners, this guide includes a catalog of common building enclosure details incorporating thermal bridges. The reported values were calculated using a 3-D finite-element analysis (FEA) heat transfer software package developed by Siemens PLM Software. The catalog includes multiple roof details, two of which (10.1.9 and 10.1.13) incorporate exterior-insulated, low-slope, mechanically fastened roof assemblies over metal decks similar to (although not directly comparable to) the assemblies included in this study. Detail 10.1.9 includes a fastener density of 0.3 fasteners/ft² (3.4 fasteners/m²) with #10 and #14 fasteners embedded at different depths of a roofing assembly with various insulation thicknesses. Detail 10.1.13 includes a fastener density of 1 fastener/ft² (10.8 fasteners/m²) with #14 fasteners through the entire depth of the roofing assembly with various insulation thicknesses.

Significance

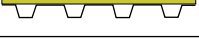
As evidenced by the range of conclusions garnered from these studies, more physical experiments and computational simulations addressing fastened roof components in their various permutations are needed to understand how thermal bridging from fasteners numerically impacts the overall thermal performance of roofing assemblies. These studies are necessary to support design efforts and the future development of building codes, industry standards, and energy performance certifications. Figures or tables containing data on the point transmittance of roof fasteners, based on their dimensional characteristics and the parameters of the roof assemblies in which they are used, such as those published within the *Building Envelope Thermal Bridging Guide*⁷ by Morrison Hershfield, allow a practical and simple way to estimate overall thermal performance. These data could, in turn, lead the roofing industry to develop more thermally efficient assembly technologies.

Table 1. Naming protocol for study

Fastener Code	Fastener Configuration
A	No fastener
B	#12 fastener, 6 in. long
Assembly Code	Assembly Type
I	Single 4 in. polyisocyanurate board
II	4 in. polyisocyanurate covered with 0.5 in. high-density polyisocyanurate cover board
III	4 in. polyisocyanurate on steel deck
IV	4 in. polyisocyanurate on steel deck covered with 0.5 in. high-density polyisocyanurate cover board
Abbreviations	Full Term
PIR	Polyisocyanurate board
HDB	High-density polyisocyanurate cover board
SD	Galvanized steel deck

Note: 1 in. = 25.4 mm.

Table 2. Assembly cases

Fastener Code	Assembly Code	Case	Assembly Components	Diagram
A	I	A-I	4 in. PIR	
A	II	A-II	0.5 in. HDB 4 in. PIR	
B	I	B-I	#12 fastener 4 in. PIR	
B	II	B-II	0.5 in. HDB #12 fastener 4 in. PIR	
A	III	A-III	4 in. PIR SD	
A	IV	A-IV	0.5 in. HDB 4 in. PIR SD	
B	III	B-III	#12 fastener 4 in. PIR SD	
B	IV	B-IV	0.5 in. HDB #12 fastener 4 in. PIR SD	

Note: HDB = high-density polyisocyanurate cover board; PIR = polyisocyanurate board; SD = galvanized steel deck. 1 in. = 25.4 mm.

METHODOLOGY

The following section summarizes the methodology used as a basis for this study in both the physical experiment and the 3-D computer simulation.

Study Setup

The roofing assembly builds in complexity, in the stepwise fashion shown in **Tables 1** and **2**.

In the B-cases, a 6 in. (150 mm) long #12 fastener penetrated the insulation layer and the top flute of the galvanized steel deck (SD), (where applicable). This resulted in an approximately 2 in. (51 mm) portion of the fastener that was exposed below the top flute of the SD. Insulation retention plates with a 3 in. (76 mm) diameter and 0.019 in. (0.48 mm) thickness were used with the fastener.

Physical Experiment

The authors tested the simplified roof assemblies as depicted in **Tables 1** and **2** in a controllable climate test chamber. The climate chamber configuration is shown in **Fig. 2**. Experimental tests were conducted in triplicate series to permit a baseline for statistical evaluation of measurements.

The climate chamber consists of a warm side (interior condition) chamber and a cold side (exterior condition) chamber. It allows for

controlling temperature and relative humidity on both sides of the test assembly and capturing temperature, relative humidity, heat flux, and air velocity measurements as needed depending on study requirements. The climate chamber was customized with an assembly frame to allow for horizontal mounting of the test assembly to include gravitational impacts. Since relatively small local heat flux differences had to be assessed, a guarded meter box approach was designed for these experiments. **Figure 3** shows an open view of the climate chamber including the meter box within the lower guard box (interior chamber).

All tests were conducted under steady-state conditions and did not consider the temperature dependence of the insulating materials. A 2×2 ft (0.6×0.6 m) area of the test assembly was monitored and the heat flux across the test assembly was measured. The exterior chamber was held at 50°F (10°C), and the interior chamber was held at 100°F (38°C), resulting in a mean insulation temperature of 75°F (24°C). For the I- and II-cases, the near-surface airflow was maintained at 50 ft/min (0.25 m/s) in the exterior chamber and 70 ft/min (0.36 m/s) in the interior chamber. For the III- and IV-cases, the near-surface airflow was maintained at 50 ft/min (0.25 m/s) in the exterior chamber and 40 ft/min (0.20 m/s) in the interior chamber. These velocities were used to create a homogeneous condition across both sides of the test assembly. Adding the SD in the III- and IV-cases changed the airflow rate in the interior chamber.

The test sequence was developed to minimize the number of times the test chamber needed to be opened and closed and the samples manipulated, and to enable the same 4 in. (100 mm) polyiso board (PIR) specimen to be used throughout an entire series of tests, thereby eliminating variation in PIR as a potential error source. The roof assemblies studied in this analysis incorporated the following modifications/simplifications from a typical roofing assembly that may be observed in the field (that is, on a construction site):

- The roofing membrane was omitted since the membrane's contribution to thermal resistance is negligible and adhering a membrane could introduce potential error between assemblies.
- The adhesive layer (for example, low-rise spray foam adhesive) was omitted between the high-density cover board (HDB) and PIR to facilitate removing the HDB between tests. Foam weatherstripping tape was applied to the top perimeter of the PIR (beneath

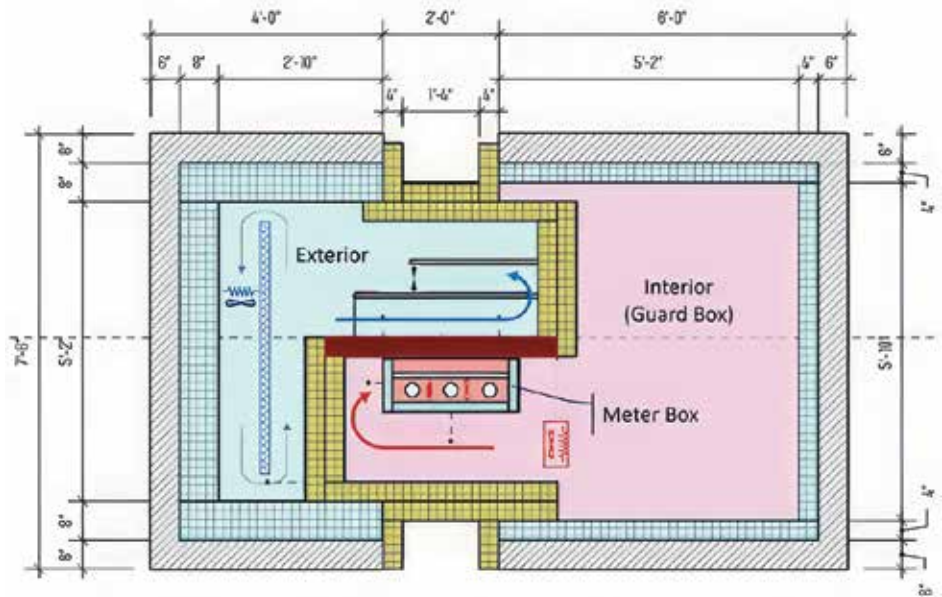


Figure 2. Climate chamber configuration for roof system testing.



Figure 3. Open view of assembly frame and meter boxes (left) and guard box with climate control (right) within the climate chamber.

the HDB) to achieve an air seal between the two layers, which resulted in an air gap of approximately 0.1 in. (2.5 mm) between the two layers.

- One layer of 4 in. (100 mm) PIR was used in lieu of multiple PIR layers to avoid discrepancies caused by imperfect contact between the layers and between staggered boards. These imperfections are not considered in computational simulations and are also difficult to replicate with each test case. The 4 in. PIR does not meet current prescriptive energy code requirements in most of the continental US (for example, per the 2021 *International Energy Conservation Code*).⁸ However, 4 in. thick boards are consistently produced and can therefore be expected to have a reliable *R*-value.
- Foam weatherstripping tape was applied to the top perimeter of the SD, beneath the PIR,

to air seal between the two layers, which resulted in an air gap of approximately 0.19 in. (4.76 mm) between the two layers. Foam flute plugs were also utilized at the open ends of the metal deck.

The above-noted modifications were included in the corresponding detailed 3-D computer simulation (see next section).

Computer Simulation

The authors performed a detailed steady-state thermal analysis of the same roof assemblies tested in the physical experiment (see Table 2) using the 3-D FEA tool ANSYS, developed by ANSYS, Inc. ANSYS simulates heat flow through materials, components, and systems based on a defined geometry and interior/ exterior environmental conditions, referred to as boundary conditions.

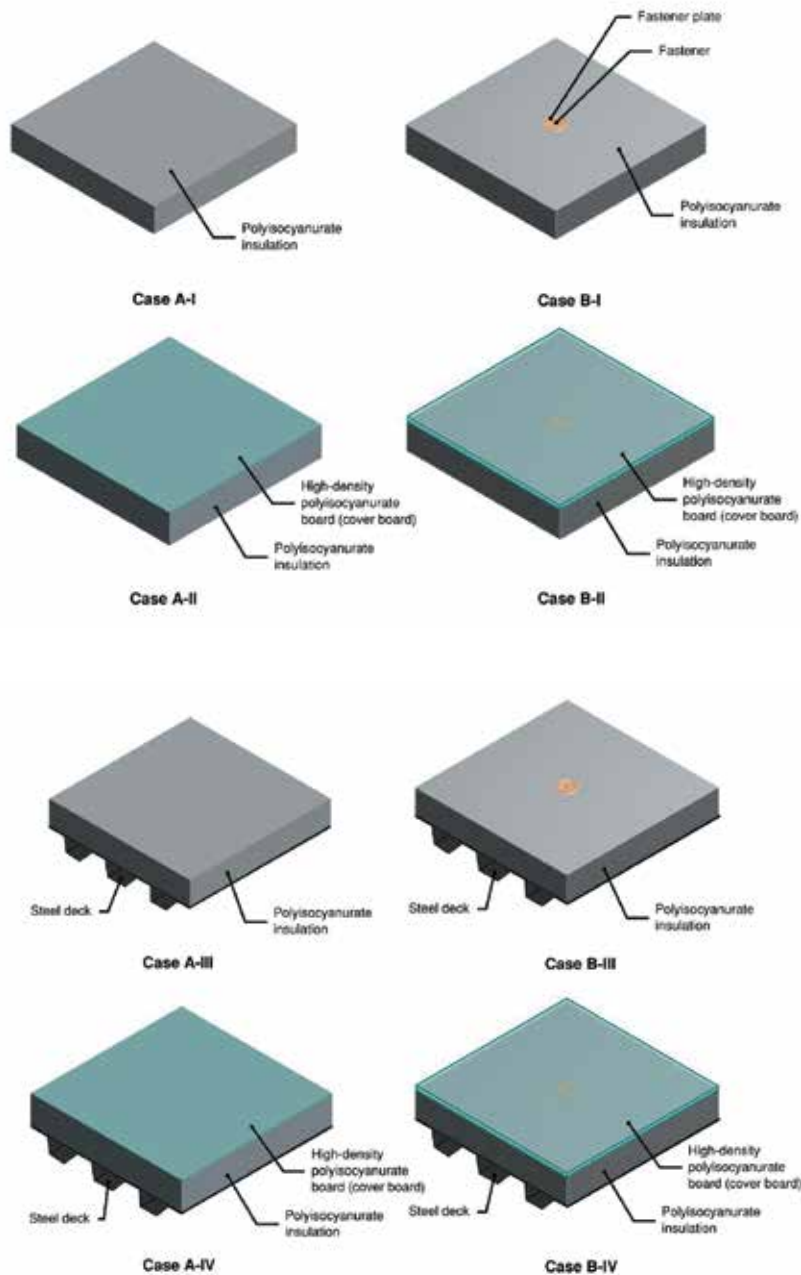


Figure 4. General geometry of three-dimensional simulated assembly configurations.

Geometry

The finite-element method utilized in the detailed ANSYS computer simulation allows for a more accurate representation of the fastener geometry than the finite-difference method used in past research (reference Related Studies above) since it can mesh irregular (that is, non-rectilinear) shapes.

The model geometry (**Fig. 4**) was developed as described in Tables 1 and 2, with the following clarifications: The fastener manufacturer provided a detailed 3-D SolidWorks model of the fastener and fastener plate geometry, including ribbed plate and fastener threads. Several minor

simplifications, which are considered to have negligible impacts on the overall heat flow, were made to the fastener threads and head to facilitate meshing.

Material Properties

The authors utilized a two-dimensional (2-D) FEA tool, THERM by the Lawrence Berkeley National Laboratory (LBNL), to determine the effective thermal conductivity of the small, enclosed air cavities within the model (for example, between the top of the insulation and the bottom of the cover board) for input into ANSYS.

Thermal conductivities and their sources for the solid model components are as follows:

- High-density polyiso board (HDB): 0.017 Btu/hr-ft-°F (0.029 W/m-K), from manufacturer's published product data
- Polyiso insulation board (PIR): 0.015 Btu/hr-ft-°F (0.026 W/m-K), from manufacturer's published product data
- Fastener and plate (carbon steel): 29 Btu/hr-ft-°F (50 W/m-K), from fastener manufacturer
- Galvanized steel deck (SD): 36 Btu/hr-ft-°F (62 W/m-K), from THERM material database
- Air cavities: vary, from THERM model

Boundary Conditions

Each case was modeled with steady-state boundary conditions applied to the outermost surfaces (**Fig. 5**). The side faces of the assembly (that is, cut surfaces at the perimeter of the assembly) were assigned as adiabatic boundary conditions, which represent boundaries across which there is no heat flow. Simulations were based on 2 × 2 ft (0.6 × 0.6 m) assembly dimensions.

The boundary conditions (indicated in **Table 3**) incorporate near-surface temperatures and air flows and the emissivity of the adjacent visible surfaces (that is, interior surfaces of the testing chamber) measured in the physical experiment. The authors matched the computer models' boundary conditions to the experimental setup rather than utilizing standard ASHRAE boundary conditions, to eliminate a possible source of difference between the experimental and computer simulation results.

To calculate the convective film coefficient, the authors followed the methodology for forced convection (utilizing external flows over a flat plate) outlined in chapter 4 of the *2017 ASHRAE Handbook: Fundamentals*.⁹ Properties of air were obtained from papers by Baumgartner et al.¹⁰ and Kadoya et al.¹¹ The convective film coefficient does not incorporate natural convection as it is expected that the size of the test chamber limits the ability for natural convection to develop.

Simulation

The simulated heat flow in ANSYS was converted into a *U*-factor (and associated *R*-value) using the projected area of the assembly in the horizontal (that is, projected-*X*) plane. **Figure 6** shows the typical temperature output from ANSYS.

RESULTS

The following section summarizes results from both the physical experiment and the 3-D computer simulation.

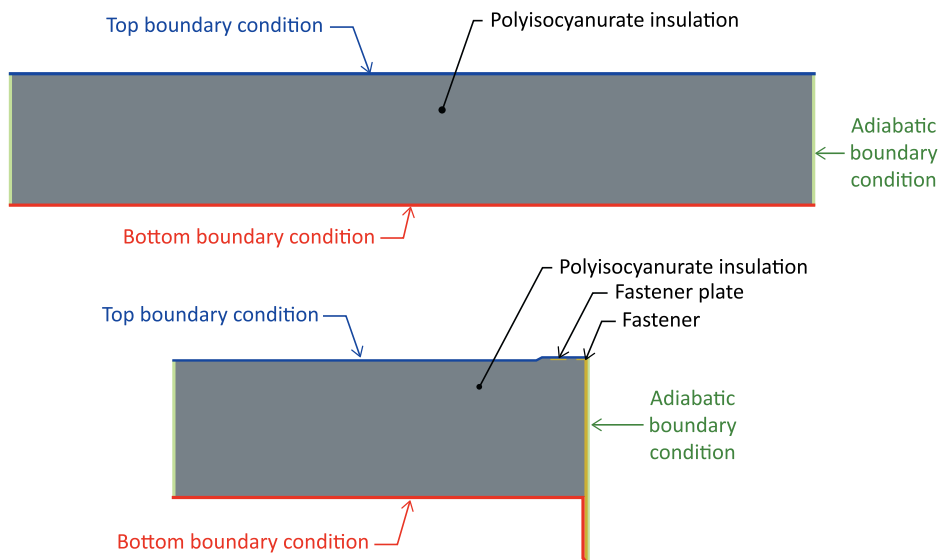


Figure 5. Example boundary conditions for cases A-I (top) and B-I (bottom).

Physical Experiment Results

Figure 7 shows the average calculated thermal resistance R -values and the range of individual test results from the three laboratory tests for each test assembly configuration. **Figure 8** shows the percent change from the A-case R -values to the B-case R -values.

The cases with no fastener (A-cases) show the following trends:

- **Case A-I to A-II:** The R -value increased by 10.8% when adding the cover board (HDB) to the PIR.
- **Case A-I to A-III:** The R -value increased by 13.5% when adding the steel deck (SD) to the PIR.
- **Case A-I to A-IV:** The R -value increased by 19.4% when adding the HDB and SD to the PIR.
- **Case A-II to A-IV:** The R -value increased by 7.7% when adding the SD to the PIR and HDB.

- **Case A-III to A-IV:** The R -value increased by 5.2% when adding the HDB to the PIR and SD.

The cases with a #12 fastener (B-cases) show the following trends:

- **Case B-I to B-II:** The R -value increased by 13.1% when adding the HDB to the PIR.
- **Case B-I to B-III:** The R -value increased by 5.4% when adding the SD to the PIR.
- **Case B-I to B-IV:** The R -value increased by 17.0% when adding the HDB and SD to the PIR.
- **Case B-II to B-IV:** The R -value increased by 3.4% when adding the SD to the PIR and HDB.
- **Case B-III to B-IV:** The R -value increased by 11.0% when adding the HDB to the PIR and SD.

The cases with no fastener (A-cases) and the cases with a #12 fastener (B-cases) show the following trends relative to one another:

- **A-cases to B-cases overall:** Adding a #12 fastener in the B-cases reduced the thermal resistance by a range of 2.2% (A-II to B-II) to 11.0% (A-III to B-III) when compared to the same condition in the A-cases with no fastener.
- **III-cases vs. I-cases:** The III-cases with PIR and an SD had a greater relative drop in thermal resistance when the #12 fastener was added (11.0%) compared to the I-cases with just PIR (4.2%).
- **IV-cases vs. II-cases:** The IV-cases with PIR, an HDB, and an SD also had a greater relative drop in thermal resistance when the #12 fastener was added (6.1%) compared to the II-cases with just PIR and an HDB (2.2%).
- **II-cases vs. I-cases:** The II-cases with PIR and an HDB had a lesser relative drop in thermal resistance when the #12 fastener was added (2.2%) compared to the I-cases with just PIR (4.2%).
- **IV-cases vs. III-cases:** The IV-cases with PIR, an HDB, and an SD also had a lesser relative drop in the thermal resistance when the #12 fastener was added (6.1%) compared to the III-cases with just PIR and SD (11%).

Computer Simulation Results

Figure 9 below shows calculated R -values from the computer simulation of each test assembly configuration, and **Fig. 10** shows the percent change from the A-case R -values to the B-case R -values.

The cases with no fastener (A-cases) show the following trends:

- **Case A-I to A-II:** The R -value increased by 10.2% when adding the HDB to the PIR.
- **Case A-I to A-III:** The R -value increased by 0.8% when adding the SD to the PIR.

Table 3. Boundary conditions used for computer simulation in ANSYS

Surface	Temperature		Convective Film Coefficient		Emissivity
	°F	°C	Btu/hr-ft ² -°F	W/m ² -K	
Bottom, warm side (I- and II-cases)	100	38	0.54	3.08	0.95
Top, cold side (I- and II-cases)	50	10	0.44	2.49	0.95
Bottom, warm side (III- and IV-cases)	100	38	0.41	2.33	0.95
Top, cold side (III- and IV-cases)	50	10	0.44	2.49	0.95
Sides, adiabatic	N/A	N/A	N/A	N/A	N/A

Note: N/A = not applicable.

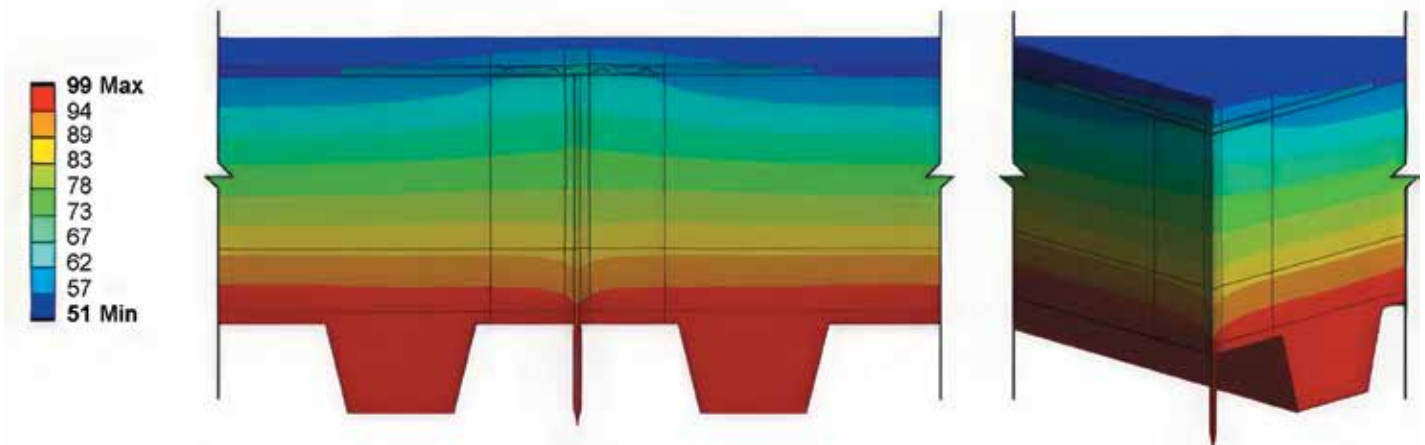


Figure 6. Color temperature output for case B-IV at fastener (section and isometric views).

- **Case A-I to A-IV:** The R -value increased by 11.4% when adding the HDB and SD to the PIR.
- **Case A-II to A-IV:** The R -value increased by 1.2% when adding the SD to the PIR and HDB.
- **Case A-III to A-IV:** The R -value increased by 10.5% when adding the HDB to the PIR and SD.

The cases with a #12 fastener (B-cases) show the following trends:

- **Case B-I to B-II:** The R -value increased by 11.0% when adding the HDB to the PIR.
- **Case B-I to B-III:** The R -value decreased by 0.4% when adding the SD to the PIR.
- **Case B-I to B-IV:** The R -value increased by 10.5% when adding the HDB and SD to the PIR.
- **Case B-II to B-IV:** The R -value decreased by 0.4% when adding the SD to the PIR and HDB.
- **Case B-III to B-IV:** The R -value increased by 11.0% when adding the HDB to the PIR and SD.

The cases with no fastener (A-cases) and the cases with a #12 fastener (B-cases) show the following relative trends to one another:

- **A-cases to B-cases overall:** Adding a #12 fastener in the B-cases reduced the thermal resistance by a range of 2.7% (A-II to B-II) to 4.6% (A-III to B-III) when compared to the same condition in the A-cases with no fastener.
- **III-cases vs. I-cases:** The III-cases with PIR and SD had a greater relative drop in thermal resistance when the #12 fastener was added (4.6%) compared to the I-cases with just PIR (3.4%).
- **IV-cases vs. II-cases:** The IV-cases with PIR, an HDB, and an SD also had a greater relative drop in thermal resistance when the #12 fastener was added (4.2%) compared to the II-cases with just PIR and an HDB (2.7%).
- **II-cases vs. I-cases:** The II-cases with PIR and an HDB had a lesser relative drop in the

Experimental R -Value per Assembly

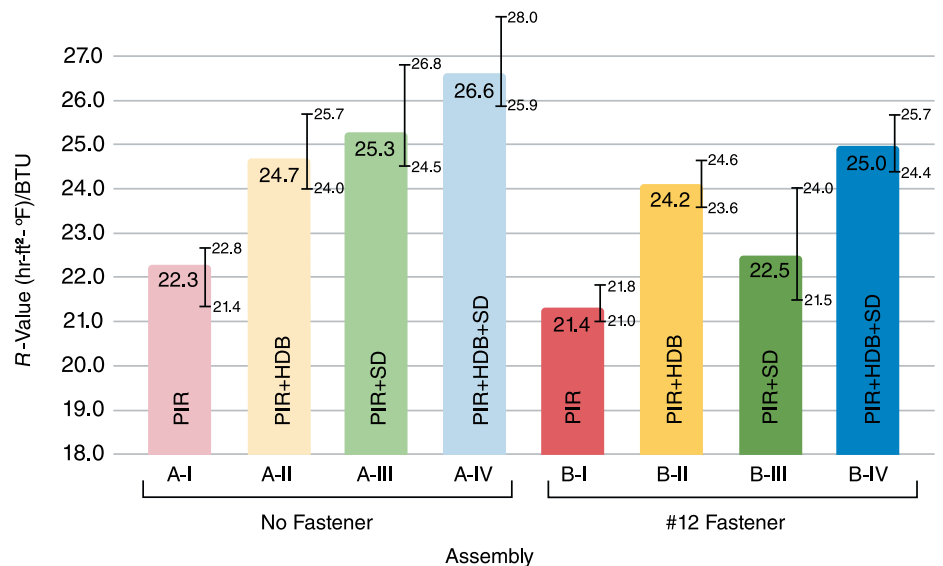


Figure 7. Physical experiment R -value for each assembly.

thermal resistance when the #12 fastener was added (2.7%) compared to the I-cases with just PIR (3.4%).

- **IV-cases vs. III-cases:** The IV-cases with PIR, an HDB, and an SD also had a lesser relative drop in the thermal resistance when the #12 fastener was added (4.2%) compared to the III-cases with just PIR and SD (4.6%).

Comparative Results

Figure 11 shows calculated R -values from the physical experiment compared to the computer simulation for each test assembly configuration, and **Fig. 12** shows the percent change from the A-cases' R -values to the B-cases' R -values for the two procedures.

The two procedures show the following notable differences for the cases with no fastener (A-cases):

- **Case A-I to A-III:** The R -value increased by 13.5% in the physical testing when adding

the SD to the PIR, while the corresponding R -value in the computer simulation stayed relatively constant (0.8% increase).

- **Case A-II to A-IV:** The R -value increased by 7.7% in the physical testing when adding the SD to the PIR and HDB, while the corresponding R -value in the computer simulation increased only slightly (1.2% increase).
- **Overall comparison:** The difference between the physical experiment results and the computer simulation results varies between 1.2% and 5.9% by case (utilizing the physical experiment data as a baseline).

The two procedures show the following notable differences for the cases with a #12 fastener (B-cases):

- **Case B-I to B-III:** The R -value increased by 5.4% in the physical testing when adding the SD to the PIR, while the corresponding

R-value in the computer simulation stayed relatively constant (0.4% decrease).

- **Case B-II to B-IV:** The R-value increased by 3.4% in the physical testing when adding the SD to the PIR and HDB, while the corresponding R-value in the computer simulation stayed relatively constant (0.4% decrease).
- **Overall comparison:** The difference between the physical experiment results and the computer simulation results varies between 0.8% and 6.7% by case (utilizing the physical experiment data as a baseline).

Generally, the physical testing and computer simulation show similar trends in the relative change in thermal resistance between the A-cases and B-cases (with the addition of a #12 fastener). However, the two procedures show the following notable differences:

- **III-cases:** In the assembly with the PIR and SD, the physical testing showed a much greater relative drop in the thermal resistance (11%) compared to the computer simulation (4.6%).
- **IV-cases:** In the assembly with the PIR, HDB, and SD, the physical testing showed a somewhat greater relative drop in the thermal resistance (6.1%) compared to the computer simulation (4.2%).

DISCUSSION AND CONCLUSIONS

In this section, the results from the previous section are discussed in detail. The discussion is divided into three sections: physical experiment conclusions, computer simulation conclusions, and conclusions related to the comparison between computer simulation and experimental results. A discussion on the comparison to past research by others (that is, related studies) is also included.

Physical Experiment Conclusions

The experimental results show that adding a fastener reduces the thermal resistance of the roofing assembly in all cases. By incrementally adding layers, the results show the following:

1. The insulating effect of HDB:

- In cases without a fastener, adding the SD to the PIR (A-III relative to A-I) has a better R-value than adding the HDB alone (A-II relative to A-I). However, in the cases with a fastener, adding the HDB to the PIR (B-II relative to B-I) is more effective than adding the SD alone (B-III relative to B-I) because the HDB reduces the thermal bridging from the fastener.
- In cases with a fastener, in assemblies with PIR and SD alone compared to PIR alone (B-III relative to B-I), there is increased

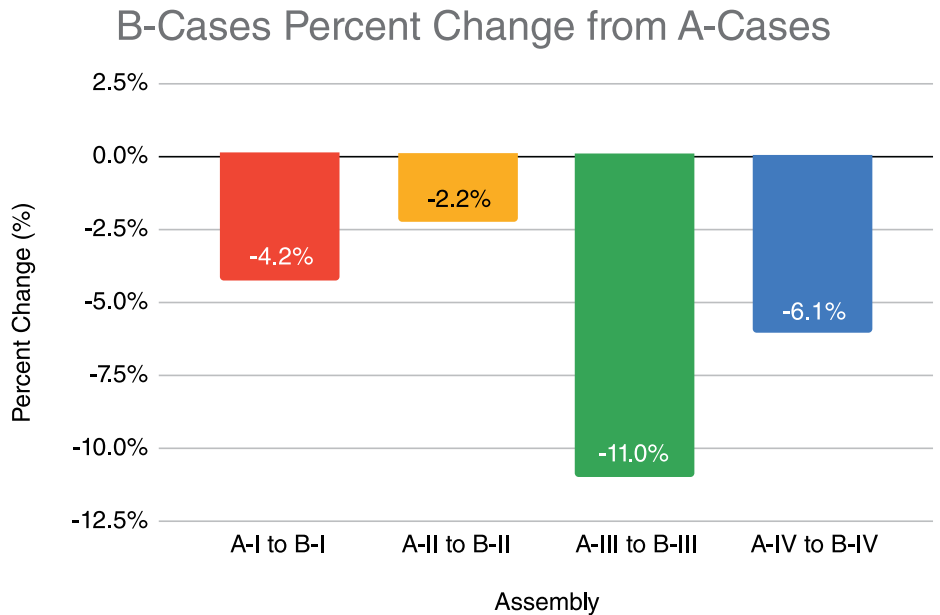


Figure 8. Physical experiment R-value percent change from A-cases to B-cases.

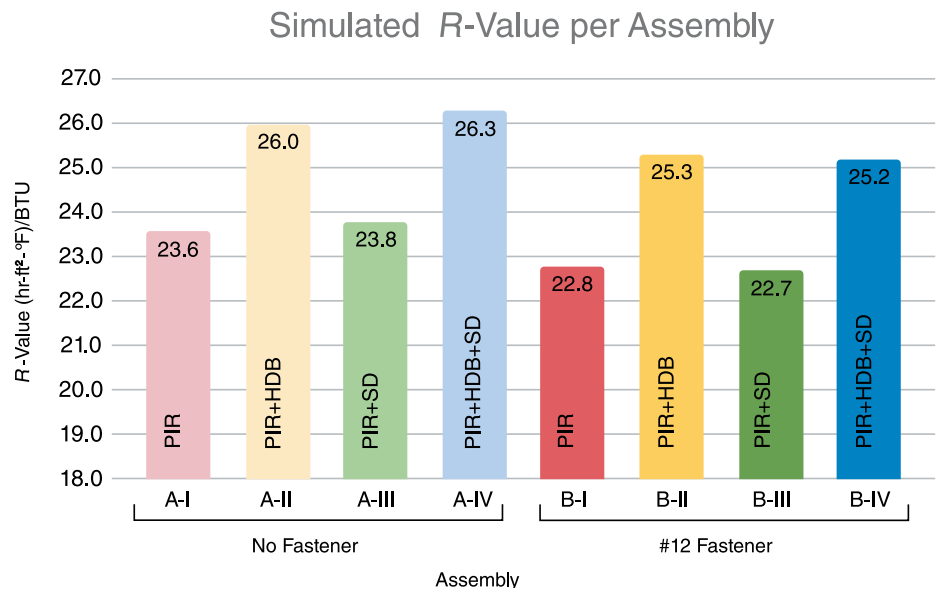


Figure 9. Computer simulation R-value results for each assembly.

radiant exchange to the interior because the SD with a fastener acts as a radiator. Adding the HDB (B-IV) insulates the fastener, increasing the fastener and SD temperature and reducing the radiant heat exchange to the interior.

- In cases with a fastener, both cases that include the HDB (B-II and B-IV) had a much smaller drop in R-value relative to their corresponding A cases than those without a HDB (B-I and B-III).
- #### 2. The insulating effect of SD air spaces:
- In cases with and without a fastener, the addition of an SD (A-III and B-III relative to A-I and B-I, respectively, and A-IV and

B-IV relative to A-II and B-II, respectively) increases the thermal resistance, which is likely due to the enclosed air pockets within the flutes, since trapped air is an insulator.

- In the cases adding an SD to PIR without a fastener (A-III), the SD with air pockets has a higher R-value than HDB and PIR (A-II). This trend is not the same when a fastener is added, as B-III has a lower R-value than B-II. The fastener may introduce enough thermal bridging to counteract the benefit of the insulating air spaces with this specific configuration.
- #### 3. The impact of SD on thermal bridging:

B-Cases Percent Change from A-Cases

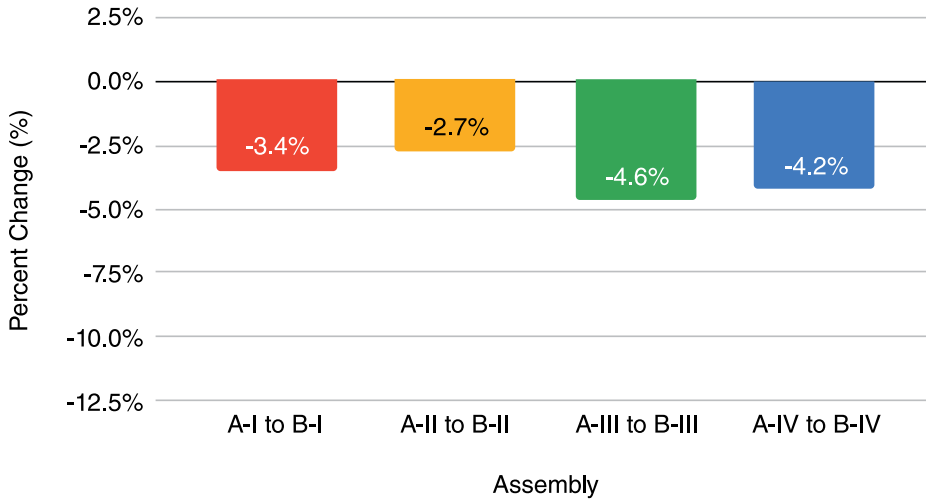


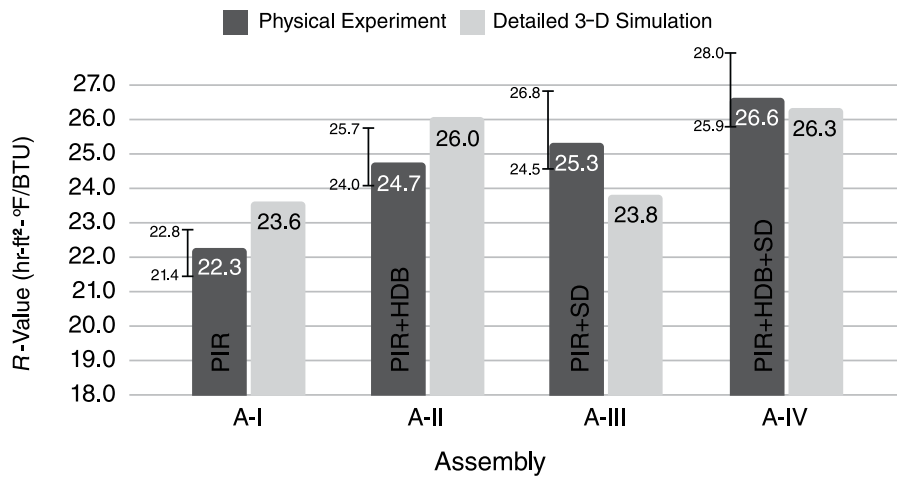
Figure 10. Computer simulation R-value percent change from A-cases to B-cases.

- The SD cases without an HDB had a greater relative drop in thermal resistance compared to their respective A-cases when fasteners were added (B-III relative to A-III) than those with PIR alone (B-I relative to A-I). This is likely because the SD acts as a thermal radiator.
- The SD cases had a greater relative drop in thermal resistance compared to their respective A-cases when fasteners were added (B-III and B-IV relative to A-III and A-IV, respectively) than did the cases without an SD (B-I and B-II relative to A-I and A-II, respectively).

In summary, the physical experiment results demonstrate that a roof assembly with an HDB adds insulating value from the board itself while also reducing thermal bridging from the fastener. Adding an SD also adds insulating value from the enclosed air pockets, but it concurrently amplifies the thermal bridging from fasteners.

It is worth noting, however, that various aspects of the experimental setup proved difficult to maintain and replicate, which likely impacted the results to an extent (as indicated by the variation of R-values across samples for each assembly reported in Fig. 7). Additional testing (that is, gathering of additional data points to serve as the basis for a statistical analysis) needs to be performed to evaluate potential outliers in the dataset.

A-Case R-Value by Procedure



B-Case R-Value by Procedure

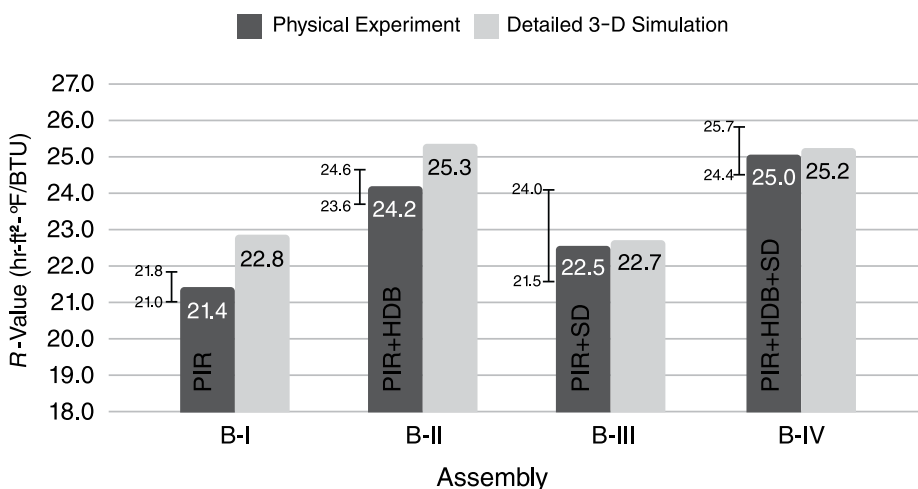


Figure 11. Comparative R-value results.

Computer Simulation Conclusions

The computer simulation results also show that adding a fastener reduces the thermal resistance of the roofing assembly in all cases. By incrementally adding layers, the results show the following:

1. The insulating effect of HDB:

- In cases without a fastener, adding the HDB to the PIR (A-II relative to A-I) is more effective than adding the SD alone (A-III relative to A-I). The same trend can be seen when a fastener is added (B-II relative to B-I versus B-III relative to B-I). This diverges from the experimental result trend for the same cases.
- In cases with a fastener and PIR, with or without SD alone (B-III relative to B-I), there is minimal difference in R-values. Adding the HDB (B-IV) insulates the fastener, increasing the fastener and SD temperature and reducing the radiant heat exchange to the interior.
- In cases with a fastener, both cases that include the HDB (B-II and B-IV) had a smaller drop in R-value relative to their

B-Case Percent Change from A-Case

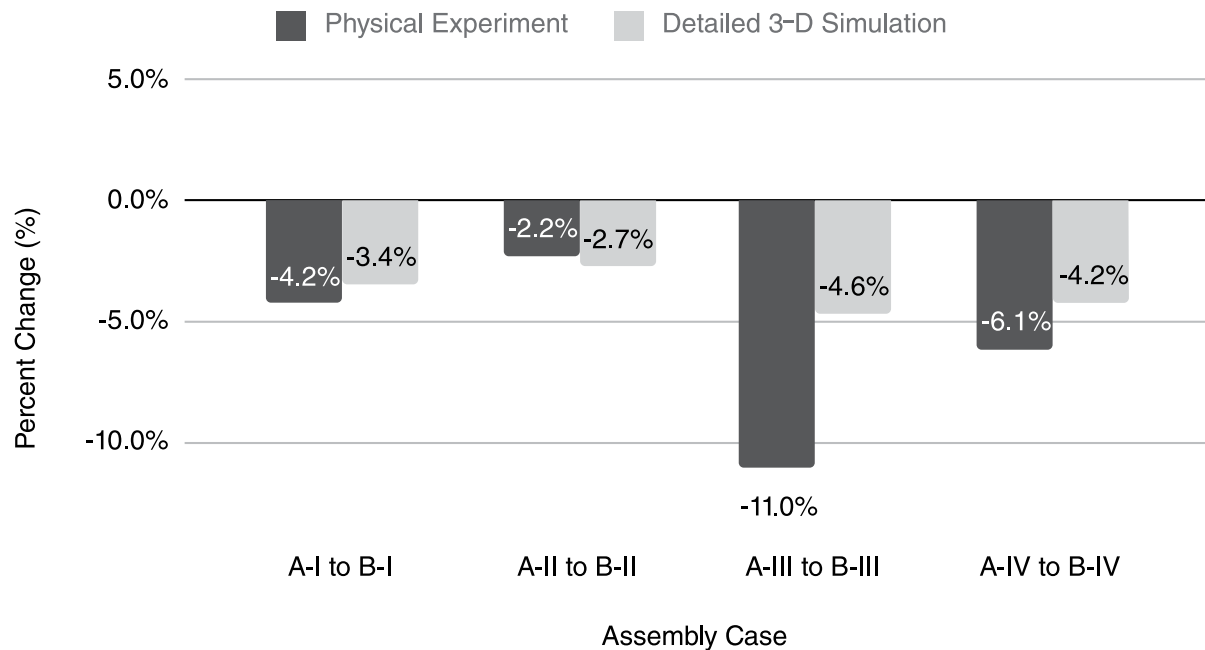


Figure 12. Comparative percent change from A-cases to B-cases.

corresponding A-cases than those without an HDB (B-I and B-III).

2. The insulating effect of SD air spaces:

- Adding the SD changes the *R*-value minimally with or without a fastener (A-III relative to A-I, A-IV relative to A-II, B-III relative to B-I, and B-IV relative to B-II). This indicates that air space modeling and contact resistance between layers requires further study. Note that the metal deck and insulation were not modeled in contact with one another since the physical experiment incorporated a small (0.19 in. [4.76 mm]) air gap between the two layers.

3. The impact of SD on thermal bridging:

- The SD cases without an HDB had a greater relative drop in thermal resistance compared to their respective A-cases when fasteners were added (B-III relative to A-III) than those with insulation alone (B-I relative to A-I). This may be because the SD acted as a thermal radiator.
- The SD cases had a greater relative drop in thermal resistance compared to their respective A-cases when fasteners were added (B-III and B-IV relative to A-III and A-IV, respectively) than did the cases without SD (B-I and B-II relative to A-I and A-II, respectively).

In summary, similar to the physical experiment, the computer simulation results demonstrate that a roof assembly with an HDB

adds insulating value from the board itself while also reducing thermal bridging from the fastener. Also, adding an SD amplifies the thermal bridging from fasteners. In contrast to the physical experiment, the computer simulation demonstrates, perhaps incorrectly, that adding an SD has minimal impact on overall thermal resistance rather than increasing the thermal resistance, indicating that the way the models account for air spaces should be further reviewed.

Comparison of the Results of Physical Experiments and Computer Simulations

When comparing the results of the physical experiments and computer simulations on a case-by-case basis, the difference between them ranges from 0.8 to 6.7%. The authors intend, through ongoing work, to review the correlations in more detail. As shown in the discussion above, some trends observed by both approaches were similar. The diverging trends that warrant further review include the following:

- The trends when adding the SD do not match. This may indicate that assumptions with air space modeling and contact resistances are inaccurate. Computer models assume each layer is in perfect contact.
- The nature of the physical experiment introduces a potential for outliers; however, it is difficult to perform statistical analyses on small sample sizes.

General Comparisons to Past Work

On the experimental side, Moletti et al.⁶ reported a 4.4% decrease in effective thermal resistance for an *R*-26 system on a steel deck with #14 fasteners penetrating a fiberglass mat gypsum roof cover board and two layers of insulation at a density of 0.25 fasteners/ft² [2.69 fasteners/m²]. While not an exact match, case B-III in this study (*R*-23.6 insulation on steel deck with #12 fasteners at a density of 0.25 fasteners/ft² [2.69 fasteners/m²] and no cover board) is similar and showed an 11.0% *R*-value reduction in the physical experiments.

On the simulation side, the results from the present study can be compared in general terms to Olson et al.'s finite-difference method simulation.³ Case B-IV in the present study is the most similar, with Olson et al.'s study utilizing a simplified representation of the metal deck, fastener, and fastener plate and including an additional gypsum substrate board between the metal deck and 4.5 in. (110 mm) thick PIR. With a #12 fastener head and plate buried below the HDB cover board, at the same fastener density as considered in this study, Olson et al. found a 5.9% reduction in effective *R*-value compared to an assembly with no fasteners. This can be loosely compared to the 4.2% *R*-value reduction found in this study for case B-IV relative to case A-IV.

General Conclusions

The authors conducted physical experiments and computer simulations in a stepwise fashion to isolate the influence of the different layers in the

assembly and to see where physical modeling and computer simulation converge and diverge. Both physical experimentation and computer simulation are simplifications of reality, and there are errors inherent in both approaches. The results of this study identify some diverging trends that warrant further analysis. The value of computer simulation, once validated by physical experimentation, is its ability to quickly extend results to a wide range of possible scenarios.

CONTINUATION

The next steps of this study include a review of the temperatures at different locations of each test assembly and the determination of point transmittances for the roof fasteners. With these data, the authors can determine more precisely where the computer simulations are diverging from the physical experiment. A sensitivity analysis can also be performed to determine the relative impact of air space modeling and the effect of contact resistances on the computer simulation results. Future work may include performing additional physical testing to produce a statistically significant sample size.

The authors also intend to perform simplified 2-D FEA evaluations, which are often used by practitioners for determining overall roof assembly thermal performance (due to increased efficiency and overall lower cost to perform the analysis), to review the potential negative consequences inherent with analyzing a 3-D problem in two dimensions.

ACKNOWLEDGMENTS

The authors would like to acknowledge the RCI-IIBEC Foundation for supporting and funding this study, OMG Roofing Products for contributing physical fasteners and plates and associated 3-D geometry of these materials for the computer simulation, and GAF for supplying polyiso and high-density polyiso boards. 

REFERENCES

1. Burch, D. M., Shoback, P. J., and Cavanaugh, K. 1987. "A Heat Transfer Analysis of Metal Fasteners in Low-Slope Roofs." *ASTM International*. West Conshohocken, PA: ASTM International.
2. Petrie, T. W., Atchley, J. A., Desjarlais, A. O., and Christian, J. E. 2000. "Effects of Mechanical Fasteners and Gaps between Insulation Boards on Thermal Performance of Low-Slope Roofs." *Journal of Thermal Envelope and Building Science*. Vol. 23, No. 4. pp. 292-317.
3. Olson, E. K., Saldanha, C. M., & Hsu, J. W. 2015. *Roofing Research and Standards Development: ASTM STP1590*. West Conshohocken, PA: ASTM International.
4. International Code Council (ICC). 2012. *International Energy Conservation Code*. Brea, CA, USA: ICC.

5. Molleti, S. and Baskaran, B. 2020. "Towards Codification of Energy Losses from Fasteners on Commercial Roofing Assemblies." *Interface*. IIBEC. Raleigh, NC: pp. 14-24.
6. Moletti, W., van Reenan, D., & Baskaran, B. 2021. "Development of Chi-Factors Towards Codification of Thermal Bridging in Low-Slope Roofing Assemblies." *Energy & Buildings*. 231, 110559. <https://doi.org/10.1016/j.enbuild.2020.110559>.
7. Morrison Hershfield Limited. 2021. *Building Envelope Thermal Bridging Design Guide v. 1.6*. Vancouver, BC: BC Hydro Power Smart.
8. ICC.
9. American Society of Heating Refrigeration and Air Conditioning Engineers (ASHRAE). 2017. *2017 ASHRAE Handbook: Fundamentals I-P and SI Editions*. Atlanta, GA: ASHRAE.
10. Baumgartner, M., R. Weigel, A. Harvey, F. Plöger, U. Achatz, and P. Spichtinger. 2020. "Reappraising the Appropriate Use of a Common Meteorological Quantity: Potential Temperature." *Atmospheric Chemistry and Physics*. Vol. 20.
11. Kadoya, K., N. Matsunaga, and A. Nagashima. 1985. "Viscosity and Thermal Conductivity of Dry Air in the Gaseous Phase." *Journal of Physical and Chemical Reference Data*. Vol. 14, No. 4.

ABOUT THE AUTHORS



SARAH RENTFRO, PE

Sarah Rentfro, PE, is a senior consulting engineer in Simpson Gumpertz & Heger Inc.'s (SGH) Building Technology group. She specializes in the design and integration of complex building enclosure systems including roofing, waterproofing, air/water barriers, cladding assemblies, and fenestration with an emphasis on performance efficiency and constructability. She is also actively engaged in SGH's Building Science practice group and has experience using various modeling software tools to simulate heat, air, and moisture flow through building enclosure systems. Her work includes new design consulting, building science modeling, construction administration, and investigation and rehabilitation of existing building enclosures.



GEORG REICHARD, PHD, PE

Georg Reichard, PhD, PE, is a professor and department head of building construction and an associate director in the Myers-Lawson School of Construction at Virginia Tech in Blacksburg, VA. His research deals with experimental and numerical methods,

simulation, and data modeling, in particular in the area of building sciences related to building enclosures and environmental systems. In his current research, he focuses on building performance, enclosure durability, disaster resilience, energy efficiency, and integrated decision-making for retrofit solutions in connection with different control strategies and building materials. Reichard holds a master's and a doctoral degree in civil engineering from Graz University of Technology, Austria.



ELIZABETH GRANT, PHD, AIA

Elizabeth Grant, PhD, AIA, is the building & roofing science research lead at GAF. She supports GAF's efforts within the commercial roofing community through engagement with design professionals, providing technical guidance in their design and

specification processes. She serves on the board of directors of the IIBEC Virginia Chapter and is a member of AIA, RICOWI, and NWIR. Before joining GAF, she was an associate professor at Virginia Tech's School of Architecture + Design, publishing papers, conducting studies, and offering courses in architectural design, environmental design research, and environmental building systems. She focuses on the building enclosure and sustainable solutions to architectural and environmental problems.



JENNIFER KEEGAN, AAIA

Jennifer Keegan, AAIA is the director of Building and Roofing Science for GAF, focusing on overall roof system design and performance. She has over 20 years of experience as a building enclosure consultant specializing in building forensics,

assessment, design, and remediation of building enclosure systems. Keegan provides technical leadership within the industry as the chair of the ASTM D08.22 Roofing and Waterproofing Subcommittee and the IIBEC Education Committee chair, and as an advocate for women within the industry as an executive board member of National Women in Roofing and a board member of Women in Construction.



ERIC OLSON, PE

Eric Olson, PE, is a principal in Simpson Gumpertz & Heger Inc.'s (SGH's) building technology group, based in Houston, TX. He specializes in evaluating and investigating building enclosures, including windows and curtainwalls, cladding

and veneer systems, roofing, and plaza and below-grade waterproofing. Olson provides design consulting services related to new building construction and building rehabilitation projects. He also specializes in forensic evaluations involving hurricane and storm-related damage assessments, design and construction claims, and litigation related to these matters. Olson has written papers and presented on several building enclosure-related topics, including thermal bridging through roofing systems.



CHERYL SALDANHA, PE, CPHD

Cheryl Saldanha, PE, CPHD leads Simpson Gumpertz & Heger Inc.'s Building Science and Passive House Practices and specializes in designing and evaluating building enclosures for new construction projects and existing building

enclosure renovations. Her experience includes curtainwall rainscreen facade, roofing, and waterproofing systems on a range of building types. Saldanha is adept at using multiple computer software packages to simulate building systems and details for thermal, condensation, whole-building energy, and daylighting analysis. She has co-chaired the New York City Chapter of the International Building Performance Simulation Association and participated on the NYC Commercial Energy Code Technical Advisory Committee for the last two code cycles. Saldanha was awarded Building Design + Construction magazine's Top 40 under 40 for 2022.



THOMAS J. TAYLOR

Thomas J. Taylor has over 25 years' experience in the building products industry, all working for manufacturing organizations in a variety of new product development roles. He is now a consultant, focused on single ply membranes and

polyiso insulation. He received his PhD in chemistry and holds approximately 35 patents.

Please address reader comments to chamaker@iibec.org, including "Letter to Editor" in the subject line, or IIBEC, IIBEC Interface, 434 Fayetteville St., Suite 2400, Raleigh, NC 27601.



Publish in



interface

IIBEC Interface is seeking submissions for the following issues. Optimum article size is 2,000 to 3,000 words, containing five to ten high-resolution graphics. Articles may serve commercial interests but should not promote specific products. Articles on subjects that do not fit any given theme may be submitted at any time.



ISSUE	SUBJECT	SUBMISSION DEADLINE
May/June 2024	IIBEC International Convention and Trade Show	January 15, 2024
July/August 2024	Restoration/Forensics	March 15, 2024
September 2024	Climate Adaptation	May 15, 2024